We are IntechOpen, the world's leading publisher of Open Access books
Built by scientists, for scientists

6,900
Open access books available

186,000
International authors and editors

200M
Downloads

154
Countries delivered to

Our authors are among the

TOP 1%
most cited scientists

12.2%
Contributors from top 500 universities

CLARIVATE ANALYTICS

BOOK CITATION INDEX

INDEXED

WEB OF SCIENCE™

Selection of our books indexed in the Book Citation Index
in Web of Science™ Core Collection (BKCI)

Interested in publishing with us?
Contact book.department@intechopen.com

Applications of Compound Nanotechnology and Twisted Inserts for Enhanced Heat Transfer

Hussain H. Al-Kayiem, Muna S. Kassim and Saud T. Taher

Abstract

Nanoadditives are a type of heat transfer enhancement techniques adopted in heat exchangers to improve the performance of industrial plants through improvement of the thermal properties of base fluids. Recently, various types of inserts with nanofluids are adopted to enhance the thermal performance of double pipe heat exchangers. In the current article, TiO_2/water nanofluid with multiple twisted tape inserts was investigated as a hybrid enhancement technique of heat transfer in straight pipes. The investigations were carried out experimentally and numerically at Reynolds numbers varied from 5000 to 20,000. Using nanofluid with 0.1% TiO_2 nanoparticles volume fraction demonstrated enhanced heat transfer with slight increase in pressure drop. Results are showing a maximum increase of 110.8% in Nusselt number in a tube fitted with quintuple twisted tape inserts with 25.2% increase in the pressure drop. However, as the article is representing a part of specified book on heat exchangers, the literature has been extended to provide sufficient background to the reader on the use of nanotech, twisted inserts, and hybrid of compound nanofluids and inserts to enhance heat transfer processes.

Keywords: enhanced heat transfer, hybrid heat transfer enhancement, multi-longitudinal vortices, multiple twisted tapes, TiO_2 nanofluid

1. Introduction

Heat exchangers (HEXs) are typical thermal systems in industrial and engineering applications. They are adopted as means of heat dissipation in a wide range of thermal processes ranging from huge scale to microscale. HEXs are involved in the power production process, chemical and food industries, electronics cooling, environmental production engineering, waste heat recovery, manufacturing industry, air conditioning, and refrigeration applications. HEXs constitute a multibillion-dollar industry in the United States alone, and there are over 300 companies engaged in the manufacture of a wide array of heat exchangers [1].

The performance of heat exchanger can significantly increase by the heat transfer augmentation techniques that lead to the reduction of heat exchanger size, as

well as operating cost reduction. Enhancement techniques can be classified either as passive or active techniques. A passive technique does not need any external power input, and the additional power needed to enhance heat transfer is taken from the available power in the system such as extended surfaces, treated surfaces, and twisted tape. Active techniques require external power such as mechanical aids and surface vibration [2].

Various methods of heat transfer enhancement are used in HEXs. These techniques are expressive to be manufactured and adopted to increase the thermal system efficiency by increasing the rate of heat transfer process and/or to reduce the size of thermal systems. They can be classified into two main categories; (i) active methods: which use an external power source; (ii) passive methods: which use several techniques without a power source such as turbulence generators (as propeller, spiral fin, twisted tapes, ribs ... etc.), or by using additives like the nanoadditives. However, in their review paper on the tape enhanced heat transfer [2], classified third enhancement techniques. They proposed compound methods, when two passive methods are used simultaneously. The method adopted in this paper is compound enhancement as twisted tapes and nanoadditives. As such, below are some backgrounds on the nanoadditives and twisted tapes to enhance heat transfer.

1.1 Nanoenhanced heat transfer

Nanoadditives are a type of heat transfer enhancement method through enhancement of the thermal properties of base materials. They may be synthesized with base fluids to produce nanofluids for thermal transport or synthesized with phase change materials (PCM) to produce nanocomposites for thermal energy storage as in [3].

Numerous works and review papers have been published in the field of nanoenhanced fluids, such as the paper of [4] who presented and compared the preparation, stability and thermophysical properties of nanofluids. It was concluded that nanofluids have, in general, better thermo-physical properties even at a very low particle concentration (typically 1.0% or less) than conventional heat transfer fluids. The only drawback is increment in the viscosity which leads to a higher pressure drop. Similar article by [5], published in 2018, has also reviewed the fabrication, stability, and thermophysical properties of nanofluids. After presenting the progress of studies on nanofluid thermophysical characterization, they identified some possible opportunities for future research that can bridge the gap between in-lab research and commercialization of nanofluids as this nanofluids are receiving large attention due to their potential usage. Reference [6], who reviewed the current scenario and future prospective of nanofluids, who also supported the conclusion of [5], ended with that the study of nanofluids has been materialized as a new field of scientific interest and innovative application. Reference [3] investigated nanofluid characteristics concerning thermal behavior in a plain tube, which showed significant enhancement rate in heat transfer with increase in nanoparticles diameter and volume concentration. Reference [7] experimented the thermophysical properties of Al_2O_3 and TiO_2 nanoparticles with distilled water and proposed parabolic equations for dynamic viscosity and thermal conductivity at specific conditions.

1.2 Enhanced heat transfer by twisted inserts

Twisted tape heat transfer enhancement mechanism is attributed to producing swirl flow in form of secondary recirculation act on the axial flow. This fluid

mechanism increases the tangential and radial turbulent components leading to higher mix fluid layers and reduces the thermal and hydrodynamic boundary layer thickness due to increase in turbulent fluctuation and combination occurring between core region and near wall region in fluid flow, which cause higher temperature gradient near the wall leading to increased heat transfer rate.

Reference [8] reported for single twisted tape insert in circular tube in which heat transfer rate increased significantly than tube without inserts, and as twist ratio decreases, the heat transfer rate and friction factor become larger. Subsequently, [9] experimented the single twisted tape insert with many different twist ratios to describe the mechanism of heat transfer enhancement and proposed correlations for Nusselt number and friction factor.

A recognized contribution to the field of heat transfer enhancement is done by the thermofluid team in University of Pretoria—South Africa. They have started their investigation on heat transfer enhancement since 2010 and since then, they published a large number of experimental and numerical investigation on the enhanced heat transfer by inserts. In 2013, [10] investigated the heat transfer enhancement in laminar flow regime in circular tubes using rib roughening and twisted tape inserts. The work is carried out experimentally, and Nusselt number and the friction factor were measured. The work concluded major finding that the center-cleared twisted tapes in combination with transverse ribs perform significantly better than the individual enhancement technique acting alone for laminar flow through a circular duct up to a certain amount of center-clearance. The reported results are useful for the design of solar thermal heaters and heat exchangers. In 2017, another two papers have been published by the same team [11, 12]. Both papers have been carried out numerically. In [11], heat transfer behavior in a tube with inserted twisted tape swirl generator is investigated numerically, for different values of the twist ratio and diameter ratio and for Reynolds numbers within the range of 100–20,000. Results have shown that the tube use of twist tape enhances heat transfer generally, but, accompanied with a higher pressure drop. Improvement of the thermal-hydraulic performance can only be observed for certain configurations and Reynolds numbers. In [12], simulations were conducted for laminar, transitional, and turbulent flow regimes for four different rib angle of attack values and for a plain tube without ribs, as benchmark case. Within the investigated range, the larger thermal performance factors are observed to occur for the intermediate Reynolds numbers. Maximum values in the range of 2.0–2.5 are predicted for the Reynolds number of 2000, where a subsequent drop to values within the range of 1.0–1.5 is found to occur for Reynolds numbers around 3000–4000, which may be attributed to the transitional effects. In 2018, a paper [13] is published by the same team, which reported results of experimental investigation of heat transfer performance of corrugated tube with spring tape inserts in turbulent forced convection in Re range of 10,000–5000. Air is adopted as working fluid. Results show that Nusselt numbers can be increased considerably, depending on pitch and spring ratios. The heat transfer enhancement to the pressure drop penalty is realized to be larger than unity for all cases. Values around 2.8 occur for cases with the smallest pitch and spring ratios. Predictive Nusselt number and friction factor correlations are proposed.

1.3 Compound nanoadditive/twisted tape enhanced heat transfer

By combining the nanofluid enhancement with inserts, [14] found that using Al_2O_3 nanoparticles with distilled water and full-length twisted tape gave a superior performance with a noticeable increment in friction loses than plain tube. Reference [15], achieved 20 and 2.5% increase in overall heat transfer coefficient and friction

factor, respectively, by using nanofluid with single twisted tape insert in double pipe heat exchanger than that without insert. Reference [16] presented an experimental analysis of the turbulent flow in tube fitted with (single, dual, triple, and quadruple) twisted tapes and nanofluid under turbulent flow conditions. The results shown that Nusselt number and friction factors increased as the number of tapes and volumetric concentration increased. Also, the increment in heat transfer rate by increase in nanofluid volumetric concentration only was higher than that of increase in twisted tape number only. It must be mentioned that the volumetric efficiency of the tube was not taken into consideration.

Reference [17] has carried out experimental and numerical investigations on similar tube flow and similar nanofluid with plain tube, tube fitted with dual plain tape inserts, tube fitted with dual twisted tapes inserts and tube fitted with dual helical screw twisted tape inserts. He concluded that, a maximum enhancement of 82.2% is achieved in the Nusselt number by using tube fitted with dual helical screw twisted tapes inserts and TiO$_2$/water nanofluid flow than that observed with the plain tube and distilled water flow. And the maximum friction factor observed for the same model of the tube fitted with dual helical screw twisted tape inserts and nanofluid are up to 17.34% than that of the plain tube. Reference [18] carried out a wide range of experimental study on the convective heat transfer enhancement using combined techniques. One of these techniques is the use of twisted tape along the whole tube length of a micro-fin tube that effectively combined the features of extended surfaces, turbulators, and artificial roughness. Nanofluids are used for improving the thermo-physical properties of the fluid. Ag-water nanofluid in a micro-fin tube with nonuniform twisted tapes insert is examined under turbulent flow. The effects of the twist ratios of nonuniform twisted-tapes of 3.0 > 2.8 > 2.6, 3.0 > 2.6 > 2.2, and 3.0 > 2.4 > 1.8, in counter and co-current flow arrangements and nanofluid concentrations of 0.007, 0.016, and 0.03% vol. are investigated. They claimed that heat transfer, friction loss, and thermal performance factors are increasing as the twist ratios are decreasing for nonuniform twisted tapes and increasing nanofluid concentrations. The optimum condition are achieved in using the micro-fin tube with a nonuniform twisted-tape in a counter-current-arrangement with twist ratios in a series of 3.0 > 2.4 > 1.8 with Ag-water nanofluid at a concentration of 0.3% vol. The enhancements are up to 112.5% for the heat transfer rate and 1.62 for thermal performance.

On other combined enhancement attempt in microchannel heat exchangers, [19] carried out experimental investigation on heat transfer for pulsating flow of GOP-water nanofluid. The effects of mass fraction of graphene oxide (GOPs) and flow pulsating frequency on heat transfer and pressure drop in a microchannel with arrayed pin-fins have been investigated. Five different mass fractions of graphene oxide nanofluids were prepared and used as working fluids. Experiments were performed under the condition that the pulsating frequency was from 1 to 5 Hz, the mass fraction was from 0.02 to 0.2%, and the average Reynolds numbers were 272, 407, and 544. The results show that the heat transfer is enhanced significantly when the frequency is in the range of 2–5 Hz. For the frequency of 1 Hz, the pulsating flow shows a negative effect on temperature uniformity. With the increase of mass fraction, the heat transfer performance is improved, while no significant change is found in pressure drop. The pulsating flow leads to a significant enhancement of pressure drop for frequency at 2 Hz. The combination of pulsating and nanofluid can obtain higher heat transfer efficiency under limited size of microchannel heat sink and low inlet Reynolds numbers. The results provided good guide for the design of microchannel heat exchangers.

Since conventional fluids, such as water, have a relatively poor heat transfer characteristic, the nanoenhancing technique opens the door to gain more benefits from these conventional fluids especially in heat transfer intensification field.

As pointed above and mentioned by many other researchers [20–23], the field of nanoenhanced heat transfer with multiple inserts is still virgin. Further experimental data are essential to support the literature, and to enhance the understanding of hydrothermal behavior in thermal systems. So far, few studies have been carried out on multiple twisted tapes with nanofluid effect on thermo-hydraulic characteristics in thermal systems.

The objective of this chapter is to scrutinize the effect of compound multiple twisted tape (TT) inserts with TiO_2-water nanofluid on heat exchange enhancement in double pipe heat exchangers. Three cases of tubes fitted with single, triple, and quintuple plain twisted tapes have been investigated experimentally and simulated numerically. In addition, two bench-mark cases have been investigated: first case is with plain tube with pure water flow, and the second case is with plain tube with nanofluid flow. Results have been manipulated and presented in terms of Nusselt number for heat transfer and friction factor for pressure drop.

2. Problem formulation

The basic geometry adopted in this investigation is a straight tube with 1000 mm length, L and 50 mm internal diameter, D. Pure tube, with pure water flow and no inserts, was considered as the benchmark case to compare the thermal enhancement and the pressure drop. The other cases were investigated with a different number of inserts and with 0.1 vol.% TiO_2/water nanofluid.

It is worth mentioning that this research meant to investigate the flow characteristics only in compound thermal and hydrodynamic in fully developed region where the entrance effect becomes insignificant beyond a pipe length of 8 times the diameter for turbulent flow [8, 14]. The fully developed region was calculated to be accomplished at 500 mm from the tube inlet.

2.1 Twisted tape inserts

Twisted tape inserts (TT) are heat transfer enhancement devices which are dividing the flow within the tube resulting in higher velocity near the tube surface. They, also, creating spiral flow creates swirl or secondary flow in the main flow which increases local velocities and promotes mixing. They are widely used over decades to generate the swirl flow in the thermal fluid resulting in increased heat transfer coefficient, with a penalty of increased pressure drop across the flow passage. Thus, reduction in the thermal system, like the heat exchangers, can be achieved. Types of TT are shown in **Figure 1a**.
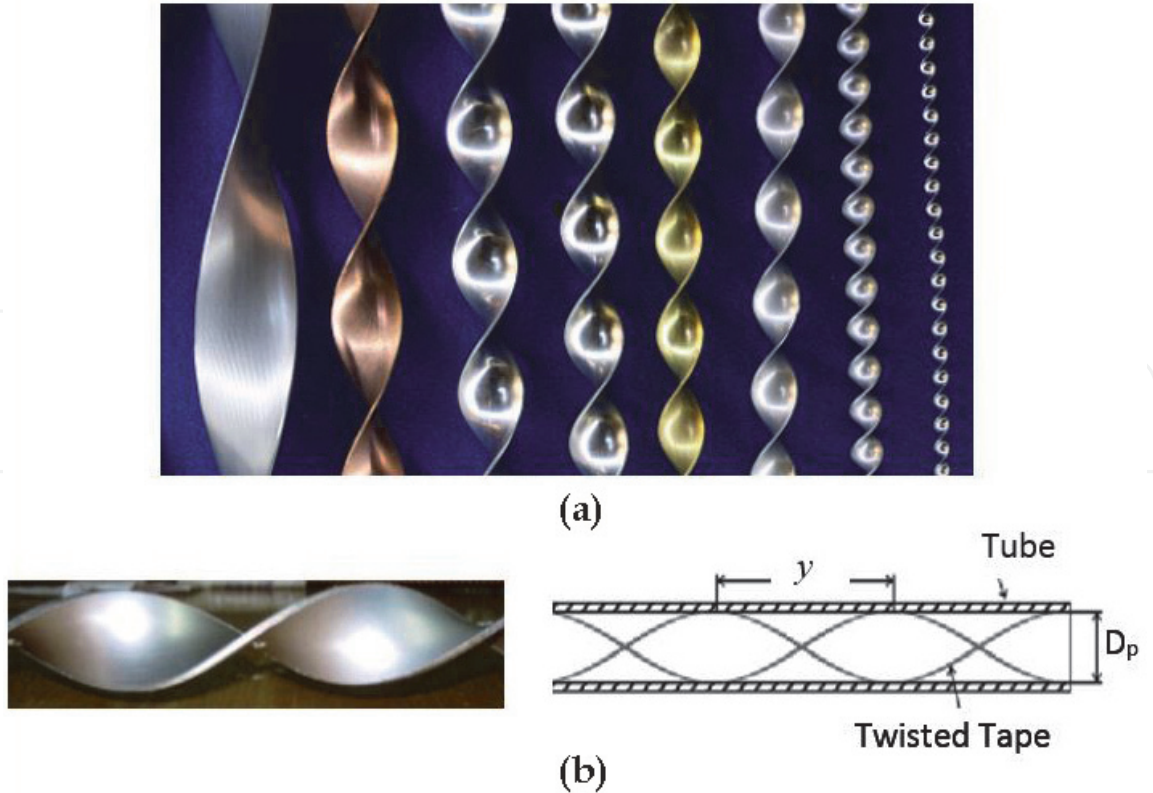
Main parameters that are commonly adopted to characterize the TT are the empty tube Reynolds number (Re), half-pitch (y), and twist ratio (Y). The main geometrical TT identifiers are shown in **Figure 1b**.

The half-pitch (y) is defined as the distance between two points on the edge of a TT, which lies down on the same plane as the TT completes 180° of revolution.
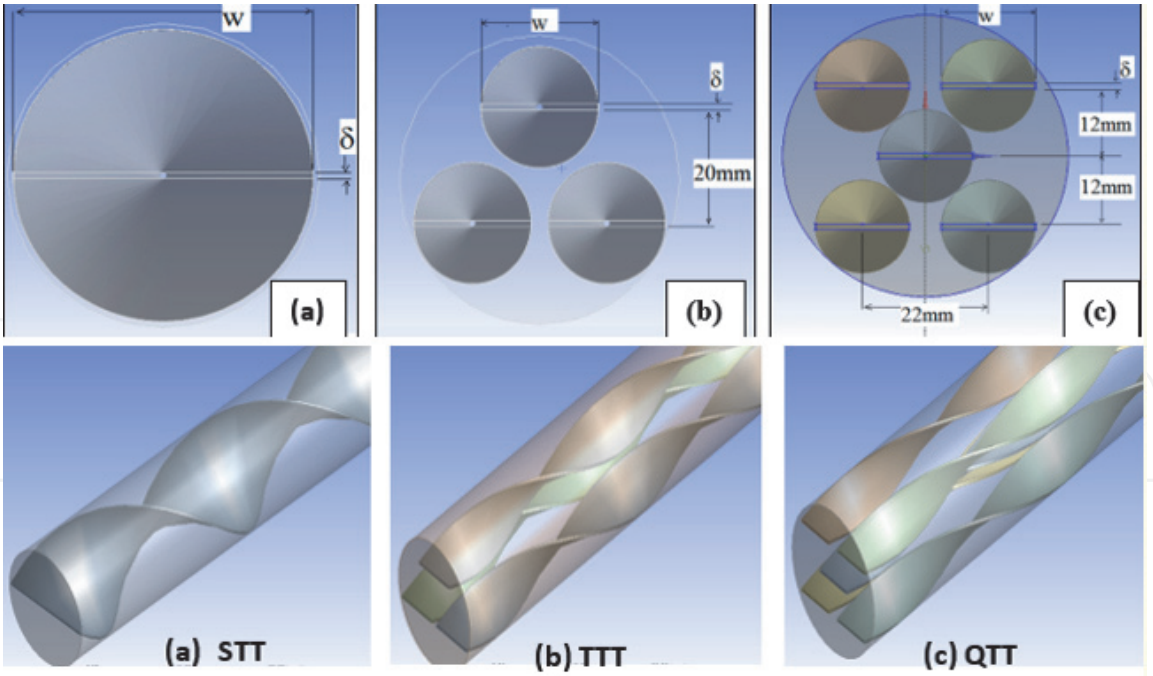
The twist ratio, Y, is defined as the ratio of the half-pitch to the internal tube diameter, $Y = y/D_p$.

Tube fitted with single twisted tape (STT), tube fitted with triple twisted tapes (TTT), and tube fitted with quintuple twisted tapes (QTT) are considered in the present experimental and numerical investigations. The schematics of cross sectional view of these models and twisted tapes and the geometries are illustrated in **Figure 2**.

The twisted tapes have the same length of the tube and has a width; L = 1000 mm, width, w (mm), thickness, δ (mm) and pitch of 180° twist, y (mm) as explained in **Table 1**. The swirl direction corresponding to tape arrangement was co-swirl flow, and all tapes were aligned to be twisted in the same direction.

Figure 1.
Twisted tape inserts; (a) different types of twisted tape inserts (courtesy of visual capitalist [24], with permission); (b) topologies of twisted tape insert.

Figure 2.
Schematic views for tubes fitted with; (a) single twisted tape (STT), (b) triple twisted tapes (TTT), and (c) quintuple twisted tapes (QTT).

2.2 Working fluids

Water was used in the primary tests to investigate the effect of inserts only on the thermo-hydraulic performance of tubes. Latterly, nanofluid of TiO_2 pre-dispersed in water was used to obtain the enhancement by both nanotechnology

Model	No. of tapes	Tape width (mm)	Tape pitch (y) (mm)	Tape length (mm)	Tape thickness (δ) (mm)	Tape material
STT	1	48	100	1000	1	Aluminum
TTT	3	21	100	1000	1	Aluminum
QTT	5	16	100	1000	1	Aluminum

Table 1.
Geometries and details of TT inserts.

	Density ρ (kg/m^3)	Specific heat (C_P) (J/kg·K)	Thermal conductivity, k (W/m·K)	Dynamic viscosity, μ (kg/m·s)
TiO$_2$	4230	692	8.4	—
Water	997	4179	0.613	855×10^{-6}

Table 2.
Properties of titanium oxide particles and water.

Property	Formula	Relation no.	Recommended by	Value
Density, ρ	$\rho_{nf} = \varphi\rho_{np} + (1 - \varphi)\rho_{bf}$	(1)	Pak and Cho [25]	1000.2 kg/m^3
Specific heat, C_P	$(C_P)_{nf} = \varphi(C_P)_{np} + (1 - \varphi)(C_P)_{bf}$	(2)	Maddah et al. [15]	4175.5 J/kg·K
Thermal conductivity, k	$k_{nf} = [1 + 3\varphi])k_{bf}$	(3)	Said et al. [7]	0.6148 W/m·K
Dynamic viscosity, μ	$\mu_{nf} = [1 + 2.5\,\varphi + 6.2\,\varphi^2])\mu_{bf}$	(4)	Batchelor [26]	857.143×10^{-6} kg/m·s

Note: φ is the percentage of volume fraction of nanoparticles.

Table 3.
Correlations of 0.1% volume of TiO$_2$-in-water nanofluid properties and predicted values.

and twisted tape inserts. In the present study, 0.1 vol.% TiO$_2$ nanoparticles of size (<50 nm) mixed with distilled water was sonicated continuously by ultrasonic vibrator generating pulses of 240 W at 40 + 4 kHz to break down any possible nanoparticle agglomeration. Nanofluid was found to be stable during tests period of tests and no intermediate mixing process considered necessary. TiO$_2$ particles and water have the considered properties illustrated in **Table 2**.
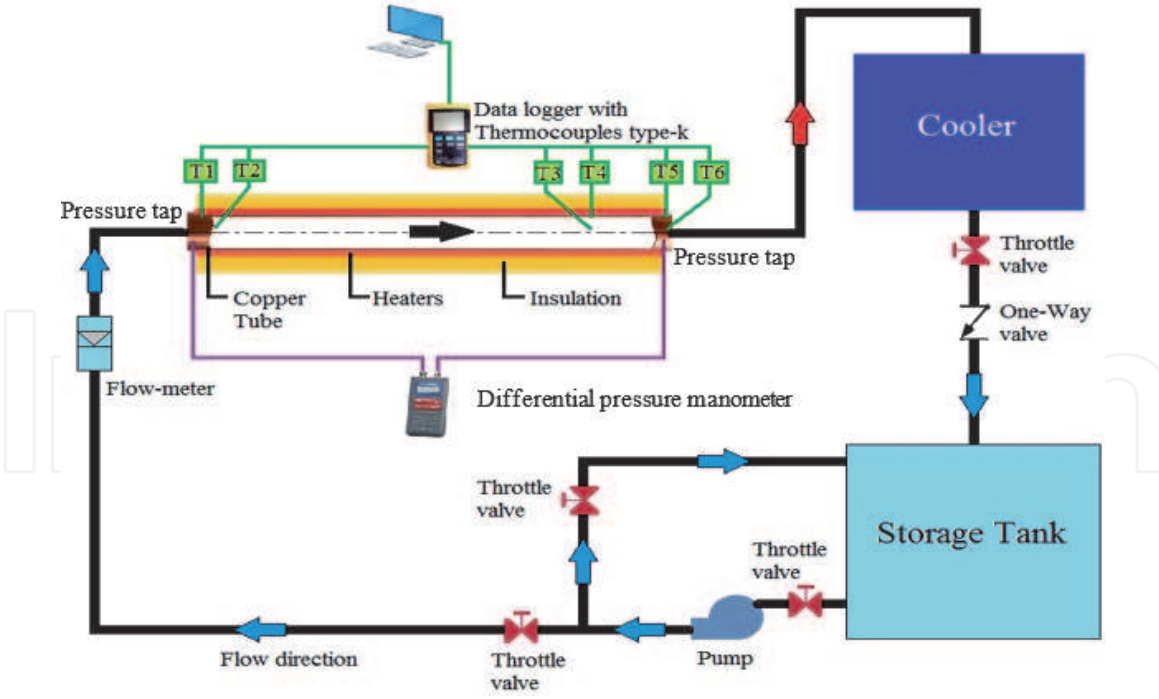
Volume concentration φ desired in this study was 0.1% for TiO$_2$/water. The thermophysical parameters are calculated for nanofluid; **Table 3** contains the popular and valid models, which were used to evaluate property values and shows values.

3. Experimental implementation

3.1 Apparatus

Experimental setup was designed and fabricated to investigate the thermo-hydraulic characteristics of the double pipe heat exchanger, as shown in **Figure 3**. The test section comprised of copper tube of 1000 mm length with inside and

Figure 3.
Schematic diagram of the experimental setup.

outside diameters of 50 and 53 mm, respectively. An electric heater with 5 kW capacity was wounded on the outer surface of the copper tube and insulated by glass-wool insulation. Thermocouples, referred to as (T1–6) in **Figure 3**, were installed to measure wall and fluid temperature at inlet, fully developed, and outlet regions. All thermocouples were calibrated before being fixed, and all were connected to the data logger to record temperature readings. A differential pressure manometer was used to measure pressure drop along the test section. The working fluid was heated inside the test section and allowed to cool by passing through a cooler (evaporative cooling system). By recirculation, the working fluid returns to the storage tank in the flow loop and then is pumped again to the test section. Flow meter was placed at the entrance of the test section to measure the working fluid flow rate. Throttle valves were incorporated to allow controlling the working fluid flow rate and for maintenance and emergency, if any. To ensure steady state condition for each run, period of 30 minutes was permitted prior to starting the measurement and data acquisition.

3.2 Verification of experimental measurements

Heat transfer in convective flow is commonly evaluated in terms of Nusselt number, Nu, as in Eq. (5).

$$\text{Nu} = \frac{h.D_p}{k} = \frac{\left[\bar{\bar{q}}\,/(T_s - T_b)\right]D_p}{k} \qquad (5)$$

Nusselt number values were validated with the experimental results of previous researches shown in **Table 4**. Values of Reynolds numbers, Re, were evaluated as per Eq. (6), as follows:

$$\text{Re} = \frac{VD_p}{v} \qquad (6)$$

where v is the mean velocity (=measured flow rate/pipe inlet cross section area), ν is the kinematic viscosity of the working fluid, and D_p is the pipe or tube diameter.

Prandtl number is considered 7.56 for water. For nanofluid, Pr is evaluated using Eq. (7), as follows:

$$\text{Pr} = \frac{Cp_{nf} \times \mu_{nf}}{k_{nf}} \tag{7}$$

The friction factor was predicted using the known Darcy-Weisbach equation (Eq. 11), for both, water and nanofluid flow, as follows:

$$f = \frac{\Delta p}{0.5 \, \rho \, V_{in}^2 \left(\frac{L}{D_h}\right)} \tag{11}$$

where Δp is the measured pressure drop over the 1.0 m pipe length. The measured values were vindicated with results gained from well-established correlations, illustrated in **Table 5**.

Correlation	Eq. No.	Suggested by	Case of HEX
$Nu = \dfrac{\left(\frac{f}{8}\right)\left(Re_{D_h}-1000\right)Pr}{1+12.7\left(\frac{f}{8}\right)^{\frac{1}{2}}\left(Pr^{\frac{2}{3}}-1\right)}$	(8)	Gnielinski, in [27]	Tube with water flow
$Nu = 0.074 \, Re_{nf}^{0.707} Pr_{nf}^{0.385} \varphi^{0.074}$	(9)	Duangthongsuk and Wongwises [21]	Tube with nanofluid flow
$Nu = 0.024 \; Re^{0.8} pr^{0.4} \times \left[1+\frac{0.769}{y}\right]^{1.1} \left[\frac{T_b}{T_s}\right]^{0.45} \left[\frac{\pi+2-\frac{2\delta}{D}}{\pi-\frac{4\delta}{D}}\right]^{0.2} \left[\frac{\pi}{\pi-\frac{4\delta}{D}}\right]^{0.8}$	(10)	Bergles and Manglik [9]	Tube with twisted tape(s) and water flow

Table 4.
Adopted correlations from the literature to predict Nusselt number used to verify the experimental results.

Correlation	Eq. No.	Suggested by	Case of HEX
$f = 0.318 \, Re_{D_h}^{-0.25}$	(12)	Blasius, in [27]	Tube with water flow
$f = \left(0.79 \ln Re_{D_h} - 1.64\right)^{-2}$	(13)	Petukhov, in [27]	Tube with water flow
$f = 0.961 \varphi^{0.052} \, Re_{D_h}^{-0.375}$	(14)	Duangthongsuk and Wongwises [21]	Tube with nanofluid flow
$f = \left[0.079 Re^{-0.25}\left[\frac{\pi+2-\frac{2\delta}{D}}{\pi-\frac{4\delta}{D}}\right]^{1.25}\left[\frac{\pi}{\pi-\frac{4\delta}{D}}\right]^{1.75}\right]\left[1+2.06\left(1+\left(\frac{2y}{\pi}\right)^2\right)^{-0.74}\right]$	(15)	Bergles and Manglik [9]	Tube with triple twisted tapes and water flow

Table 5.
Adopted correlations from the literature to predict friction factor used to verify the experimental results.

3.3 Experimental uncertainty and errors

The used instruments were well calibrated, and the margin of error and uncertainty of each instrument were evaluated.

- Thermocouple type-K used in this study to measure temperature of surfaces. Thermocouple type-K probes were used to measure the fluid temperature. All thermocouples and probes were calibrated and certified by the Central Organization for Standardization and Quality Control (COSQC)—Baghdad—Iraq [certificate number 734/2016 dated 30 Oct. 2016]. Mean uncertainty within the temperature measurement in the experiment was ±0.63°C.

- Flow meters type LZS-25 used to measure the flow rate of heat transfer fluids were calibrated using a scaled container and time recording technique, which is well identified as a standard procedure for flow meter calibration. The relative uncertainty of flow measurement was ±2.34%.

- Differential manometer was calibrated against another certified manometer type Lutron (PM-9100). The relative uncertainty was ±2.1%.

- The two pressure gauges were calibrated and certified by the Central Organization for Standardization and Quality Control (COSQC)—Baghdad—Iraq [certificate number PRE/918/2016 dated 06 Oct. 2016]. Max uncertainty was ±0.012 bar.

The possible error in the prediction of Re and Nu was estimated. The uncertainty in Re values was estimated by Eqs. (16)–(18) using the uncertainties of the measuring instruments used for measurements of relevant variables in Re:

$$Re = \frac{4 \dot{m}}{\pi \mu d} = \frac{4 \rho \dot{V}}{\pi \mu d} \tag{16}$$

$$\Delta Re = \left[\left[\left(\frac{\sigma Re}{\sigma \dot{V}} \right) \bullet \dot{V} \right]^2 + \left[\left(\frac{\sigma Re}{\sigma d} \right) \bullet d \right]^2 \right]^{0.5} \tag{17}$$

Getting,

$$\Delta Re / Re = \left[\left[\left(\frac{\Delta \dot{V}}{\dot{V}} \right) \right]^2 + \left[\left(\frac{\Delta d}{d} \right) \right]^2 \right]^{0.5} \tag{18}$$

= 0.0665 or 6.65%.

Uncertainty in Nu values was estimated by Eq. (19) using the uncertainties of the measuring instruments used for measurements of relevant variables in Nu, as

$$\Delta Nu / Nu = \left[\left[\left(\frac{\Delta h}{h} \right) \right]^2 + \left[\left(\frac{\Delta d}{d} \right) \right]^2 \right]^{0.5} \tag{19}$$

= 0.0625 or 6.25%

4. Computational methods

4.1 Numerical simulation and conditions

The numerical analyses included single phase flow based on steady and three dimensional continuity; momentum and energy equations were performed using the ANSYS-Fluent commercial code. RNG *k-ε* model was chosen to solve the considered cases because the effect of swirl on turbulence is included in this model, which enhances the accuracy of swirling flows.

4.2 Boundary conditions

The thermo-fluid process in the current simulated was solved as steady, incompressible, and 3D flow. The following was adopted to set the boundary conditions for the simulation:

- The flow was considered as internal flow under uniform heat flux condition for all cases with $\bar{\bar{q}}$ = 30,000 W/m^2.

- No slip condition was also applied to the tube wall.

- Results are considered only at the fully developed region ($L > 10D_p$).

- Water and 0.1 vol.% TiO$_2$/water are considered as the working fluids, and calculations for the thermal properties are done at the inlet temperature of 300 K, as in **Tables 2** and **3**.

- The nanofluid was considered as a single-phase fluid with changed physical parameters as density, thermal capability, thermal conductivity, and viscosity.

- All cases were investigated within the turbulent flow regime studied with a range for Reynolds number of 5000–20,000.

- The hydraulic diameter at each inlet and outlet has the same value.

- At the outlet, a pressure outlet condition was used, and the gauge pressure is set to zero.

- Turbulence intensity obtained from the expression recommended by [28].
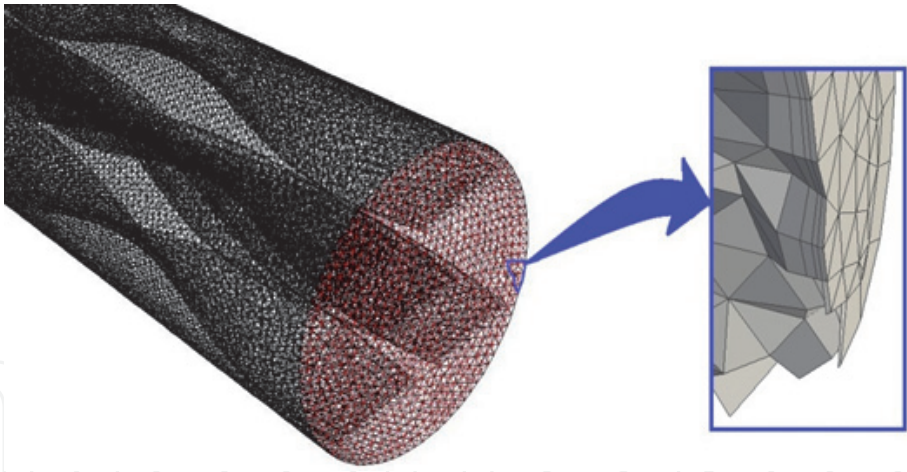
$$T.I. = 0.16\,Re_{D_p}^{-0.125} \qquad (20)$$

Other flow quantities are extrapolated from the interior domain by the solver in Fluent software. The SIMPLE (Semi-Implicit Pressure Linked Equations) algorithm were chosen as solver method. In addition, a convergence criterion of 10^{-5} was used for energy and mass conservation of the calculated parameters.
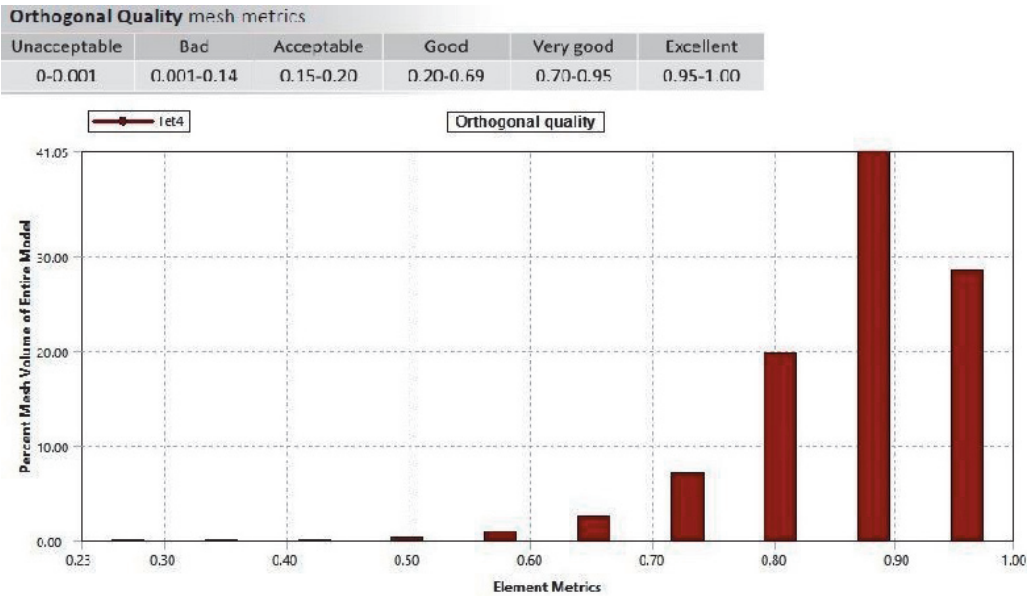
4.3 Grid generation

To avoid blurred curved areas, tetrahedral cells are used for meshing the computational domains, as shown in **Figure 4**. Mesh, with around 3,000,000 elements, was decided to represent the domains for the current simulation.
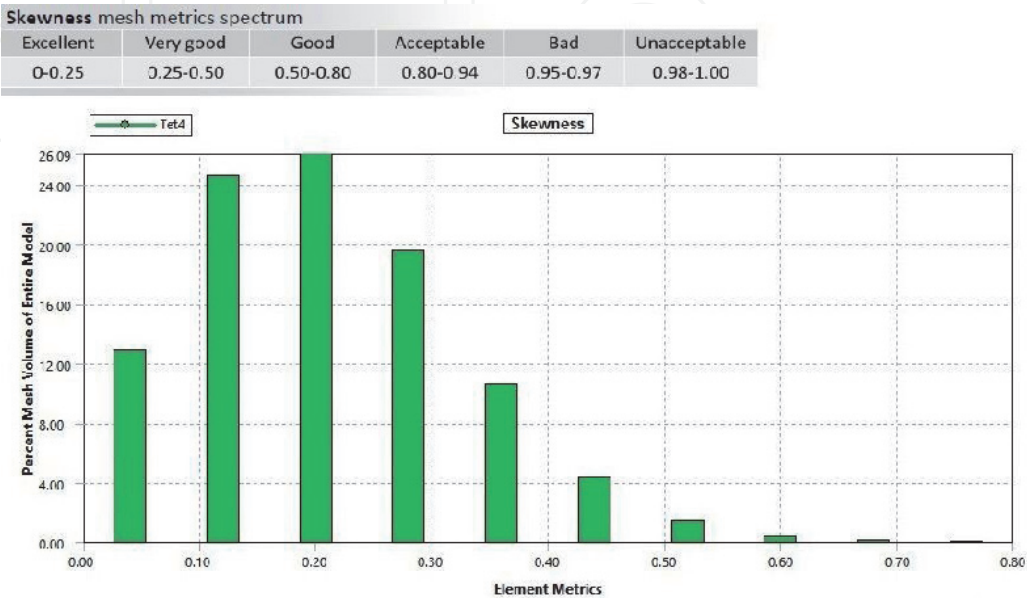
Figure 4.
Tetrahedral mesh cells for the case of QTT with enlarged small cut for clarification.

Orthogonal Quality mesh metrics					
Unacceptable	Bad	Acceptable	Good	Very good	Excellent
0-0.001	0.001-0.14	0.15-0.20	0.20-0.69	0.70-0.95	0.95-1.00

Figure 5.
Mesh cell orthogonal quality metrics.

Skewness mesh metrics spectrum					
Excellent	Very good	Good	Acceptable	Bad	Unacceptable
0-0.25	0.25-0.50	0.50-0.80	0.80-0.94	0.95-0.97	0.98-1.00

Figure 6.
Mesh cell skewness quality metrics.

The same way that element numbers in the mesh are important, mesh quality has a remarkable role in the numerical solution accuracy. Grid quality is commonly identified through orthogonal quality and skewness. Orthogonal quality describes how much the mesh criteria are within the correct range that is valid for physical value prediction. Orthogonal quality is presented in **Figure 5** for the grids performed to represent computational domains. The average orthogonal quality value gained in the present numerical procedure, of 0.8563, is within a very good quality range. Skewness determines how the generated cells are close to the ideal configuration and it governs solution ability to converge, as illustrated in **Figure 6**. The average skewness value of depended grids of 0.22288 is within excellent simulation range.

5. Results and discussion

The presentation and discussion of results are not based on sub-sectioning the numerical and experimental results. Instead, the results are sub-sectioned based on the hydrothermal parameters, like the velocity, pressure, and thermal performance.

5.1 Hydrodynamics analysis

The hydrodynamics analysis of the flow within internal conduits includes the velocity and pressure structures.

5.1.1 Velocity field analysis

The flow structure in the pipe is characterized by analyzing the velocity field and the pressure distribution in the flow domain. In the current work, there are four different geometrical configurations including plane pipe flow and another three cases with single, triple, and quintuple twisted tape inserts inside the pipe. CFD is a powerful tool to provide flow visualization and assist in the analysis of the flow field structure. Fields of velocity, predicted by computational simulation, in case of water flowing are depicted in **Figure 7**. The velocity contours shown are taken for

Figure 7.
Velocity contours and streamlines of water flow for; (i) PT, (ii) STT, (iii) TTT, and (iv) QTT.

Re = 5000 and at different axial locations in the fully developed region. As can be seen in **Figure 7**, frame ii, the velocity is increasing by 50.0% for STT higher than PT. This happens due to secondary flow caused by twisted tape geometry, which increases mean velocity by changing flow type from linear motion to swirl motion and also due to reduction in hydraulic diameter which leads to increase in velocity at constant Reynolds number and the reduction in hydraulic diameter causing a decrease in flow cross sectional area, which resulted in an increment in mean velocity value to satisfy equation of continuity (the rate of mass enters a system is equal to the rate of mass leaves the system).

For TTT and QTT, the velocity increased by 13.3 and 27.4% higher than STT due to narrowing the flow passages. Swirl motion and turbulence fluctuation are also increasing by increases in tape number due to multi-passage flow interactions. In addition, the tapes are breaking the flow field uniformity, and mix fluid flow layers between near wall region and core region lead to the appearance of many regions of high velocity; high velocity region in plain tube appears only at the core of it, which increases as the number of twisted tape increases, and that fission leads to increase in average velocity of fluid flow.

Longitudinal vortices in flow fields are shown in **Figure 8**; it was found that the number of vortices generated in the flow equals the number of twisted tapes and formed around it.
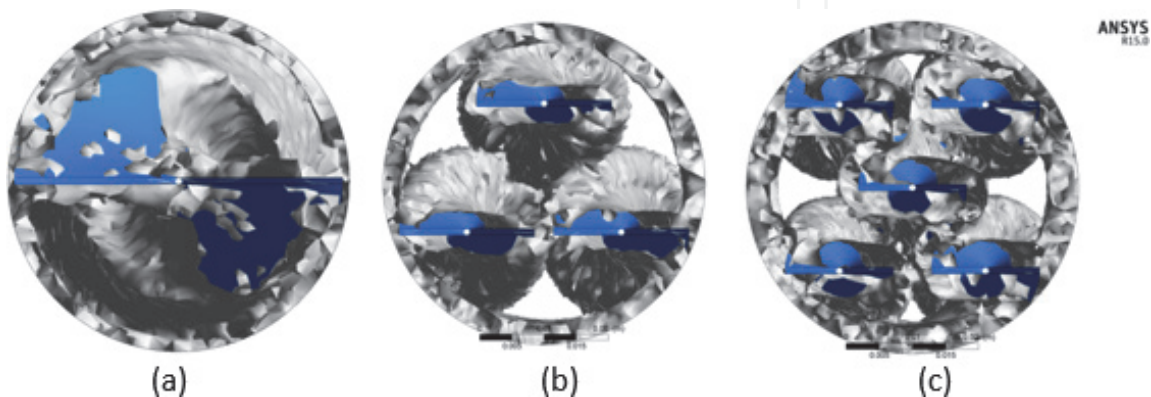
Apparently, the velocities of the nanofluid are nearly the same as those of water under the considerable nanoparticle volume fraction, which discloses that nanofluid will not require an added disadvantage over pumping power.

5.1.2 Analysis of pressure field and pressure drop

As a fluid flows through the tube, there will be a pressure drop due to the shear drag at the contact wall in addition to the pressure required to pump the fluid inside the tube which is in tube with inserts higher than those without. The main determinants of pressure drop are fluid viscosity and fluid velocity. Pressure contours are illustrated in **Figure 9** for the computational domains considered at Reynolds number 5000 for water flow and on longitudinal revolution surface along the axial direction.
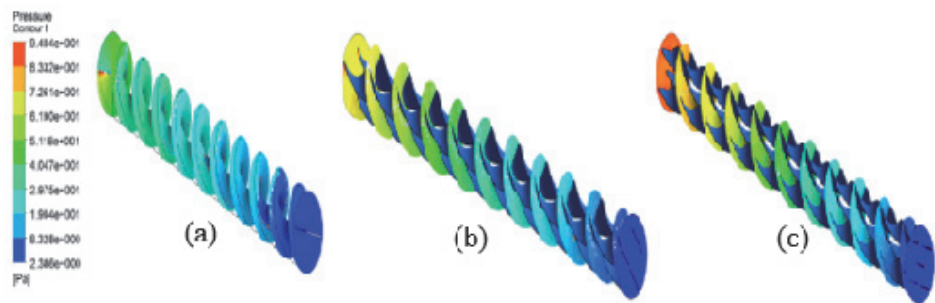
In the case of STT, **Figure 9**, frame a, pressure drop is 98.7% higher than in PT due to the fact that twisted tape insert increases frictional shear forces within the surface area of the inserts.

Figure 10 presents the predicted pressure drop for all simulated cases including pure tube and tube with single, triple, and quintuple twisted tape inserts with water

Figure 8.
Longitudinal water vortices for tube fitted with; (a) single twisted tape, (b) triple twisted tapes, and (c) quintuple twisted tapes.

Figure 9.
Pressure contours for a longitudinal revolution surface along the computational domains of water flow; (a) STT, (b) TTT, and (c) QTT.
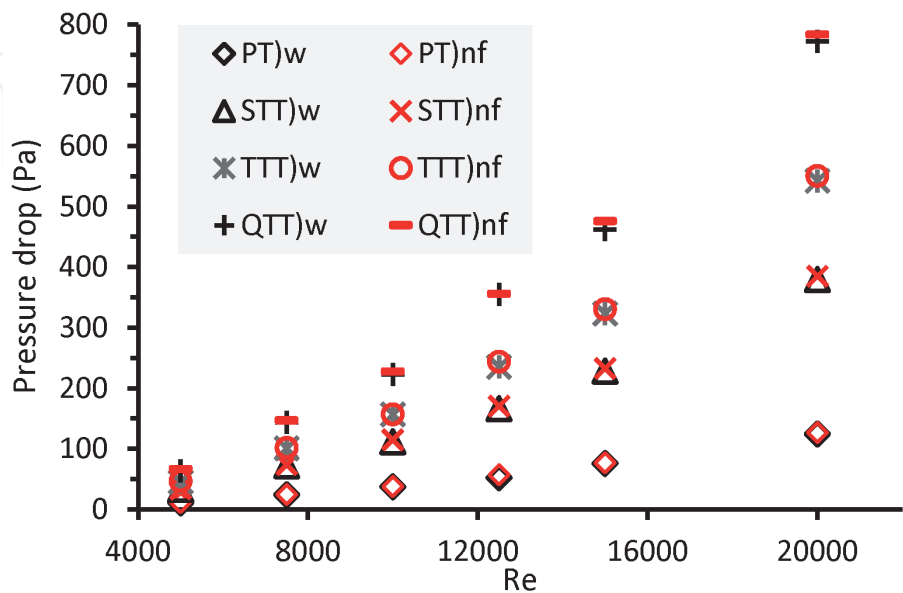
flow and with nanofluid flow. The pressure drop in TTT and QTT is 31.2 and 64.5% higher than STT, respectively. This is due to swirl motion achieved by each one of them, where the secondary motion generated by twisted tapes have an effect on velocity proportionally, where velocity gradient effect on shear forces acting on fluid flow causes pressure drop.

Pressure drop increases slightly by using nanofluid at 0.1 vol.% TiO_2. The numerical results show a percentage difference between water and nanofluid up to 3% for the same model investigated. However, experimental results for pressure agree well with those calculated numerically with a maximum divergence of 6.8%. It is obvious, from **Figure 10**, that pressure drop of water and for nanofluid increases with increasing Reynolds number. The small increase in pressure drop of nanofluid than water illustrates that using nanofluids with higher particle volume fraction may cause small penalty in pressure drop.

5.1.3 Friction factor

The friction factor is influenced by velocity variation, pressure drop, and contact surface topologies with the fluid flow. The models were examined numerically and experimentally in Reynolds number range varying from 5000 to 20,000.

The experimental results of the friction factor are reasonably matching with the results obtained from correlations 12 and 13 for the plain tube with water flow with
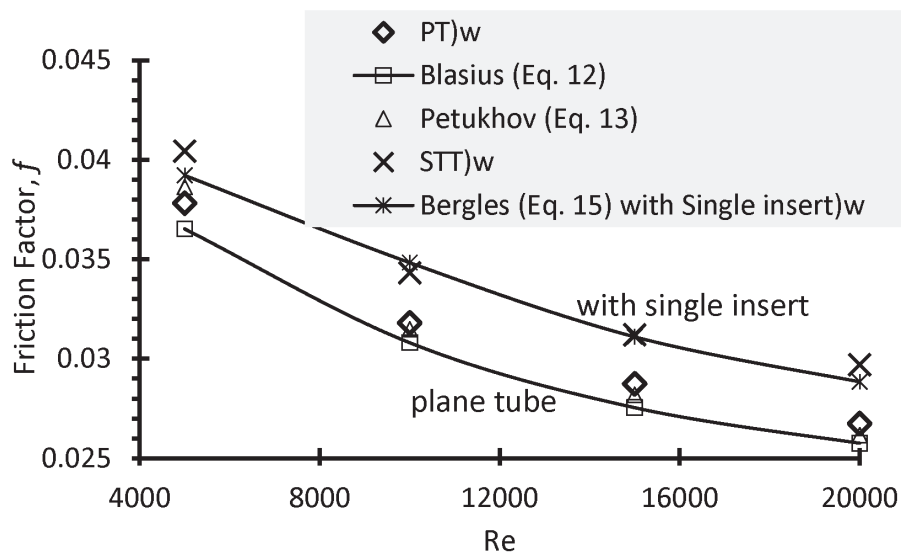

Figure 10.
Simulation results of pressure drop obtained from water (w) and 0.1 vol.% TiO_2/water nanofluid (nf) for different inserts at various Reynolds numbers.
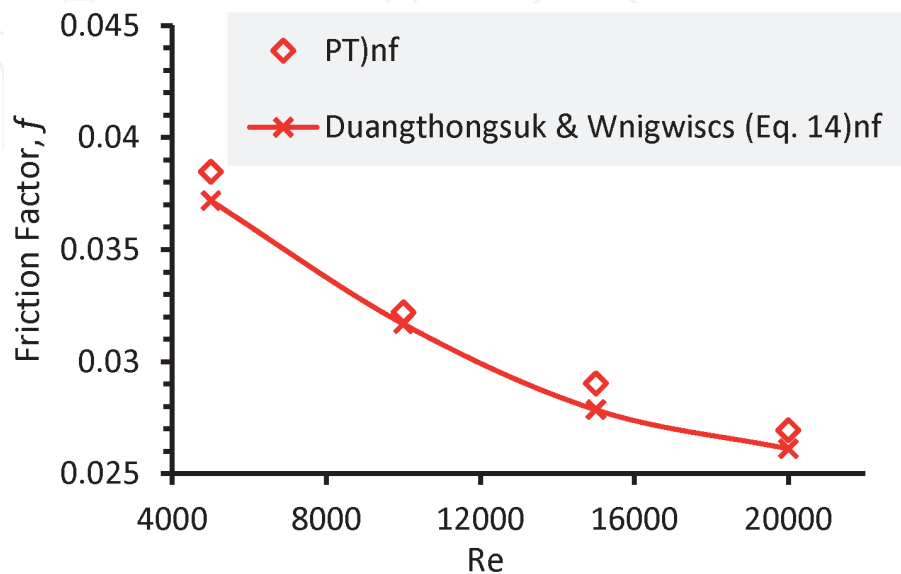
a maximum deviation of 4.1%. Further verification was carried out by comparing the experimental results of the friction factor of single TT insert in the tube with water flow by comparison with the results gained by a correlation developed by Bergles, as in Eq. (15). The maximum deviation was 3.0%. The verification results are shown in **Figure 11**.

Measured friction factors coincide well with the calculated values from correlations of validation. As the fluid velocity increases, the friction factor decreases. Therefore, friction factor decreases with Reynolds number increasing. This is because Reynolds number increases the momentum, overcomes the viscous force of the fluid, and consequently lowers the shear between the fluid and the tube wall.
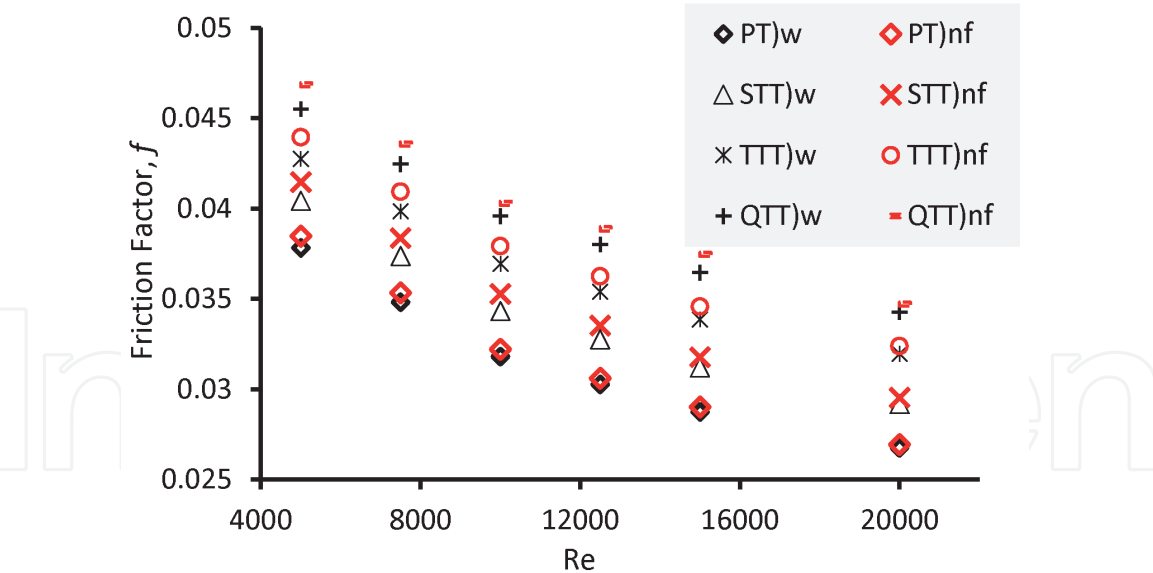
Reference [16] developed a correlation for the friction factor prediction for nanofluid flow in a plain tube, shown as Eq. (14). Comparison between the predicted results by Eq. (14) and the experimental results in the current investigations are shown in **Figure 12**. Good match between the experimental and empirical

Figure 11.
Verification of experimentally measured friction factors and those predicted from; (a) PT with water flow and prediction by Blasius (Eq. 12) and Petukhov (Eq. 13); (b) STT with water flow and prediction by Bergles (Eq. 15).

Figure 12.
Verification of experimentally measured friction factors and predicted by Duangthongsuk and Wongwises (Eq. 14) for 0.1 vol.% TiO$_2$/water nanofluid flow in plain tube.

Figure 13.
Experimental measurement results for the friction factor verses Reynolds number for plain tube and tubes with single, triple, and quintuple twisted tape inserts of flow cases of water flow and 0.1 vol.% TiO$_2$/water nanofluid flow.

values has been achieved. Within the tested range of 5000–20,000 Re, the correlation shows overprediction of around 2.0–3.0% in the friction factor values compared to the experimental results.
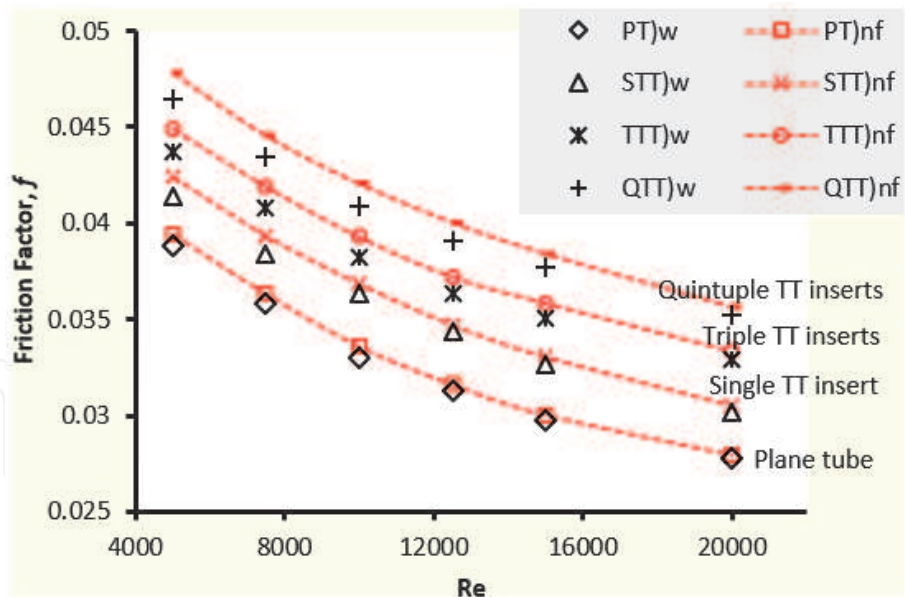
The variations of the friction factor with Reynolds number for the tubes with different twisted tape inserts, with flows of water and nanofluid, are compared in **Figure 13**. The friction factors of the nanofluids are slightly higher than those of the base liquid. The tube fitted with plain twisted tape inserts (STT) when water flow has friction factor of 6.6–8.7% higher than plain tube. This is attributed to the flow blockage and swirl flow due to tape insert; for the same case, friction factor increases by 1.2–2.4% using nanofluid.

The additional dissipation of pressure of the fluid caused by the fluid disturbance due to increase of tape number results in an increase in pressure drop, which causes increase of friction factor. As the number of inserts increases, the pressure drop significantly increases. For water flow, the friction factors of TTT and QTT are 12.2–17.74% and 18.428–24.65% higher than that in plain tube. For nanofluid flow, the friction factors of TTT are 13.3–18.4% and for QTT are 19.6–25.2% higher than that in plain tube.

Results of predicted friction factor from the numerical simulation show the same trend as of the experimental ones, where differentiations between results within 6.04% are considered as an acceptable limit. Numerical simulation results of the friction factors for cases of inserts using water and nanofluid are shown in **Figure 14**. All cases demonstrated a slight increase in the numerically predicted friction factor values when 0.1 vol.% TiO$_2$ is used as working fluid. This is attributed to the slight increase in the viscosity of the nanofluid compared to the viscosity of pure water.

5.2 Thermal analysis

The heat transfer enhancement, in terms of Nusselt number, is influenced by velocity variation, friction factor, nanoparticles volume fraction, twisted tape dimensions, and other parameters. The four models were examined experimentally and numerically within Reynolds number ranging from 5000 to 20,000. The
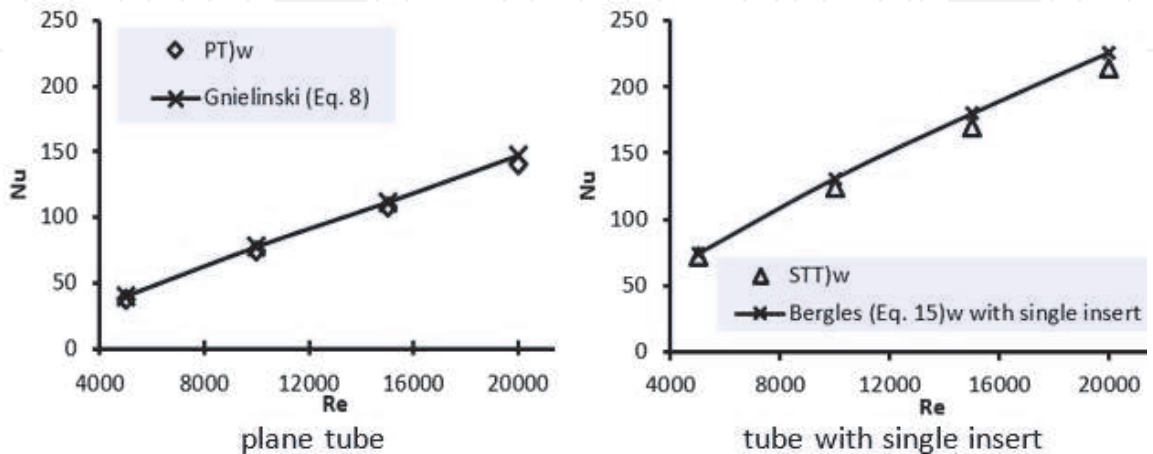
Figure 14.
Numerical simulation results of the friction factor versus Reynolds number for plain tube and tubes with single, triple, and quintuple twisted tape inserts of flow cases of water flow and 0.1 vol.% TiO₂/water nanofluid flow.
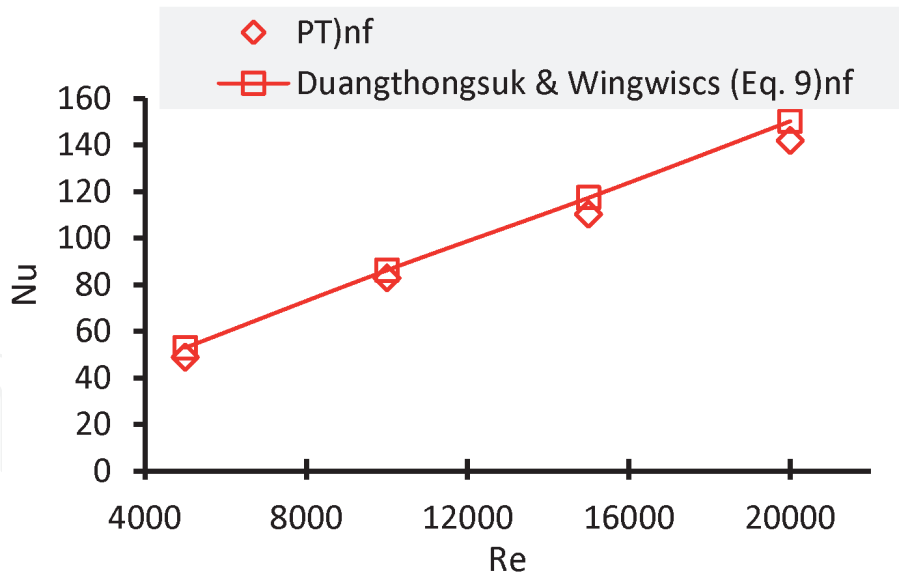
measured thermal parameters were verified by comparing the measurement results with well-established correlations to predict Nu. The verification results are shown in **Figure 15a** and **b**. The experimental results are matching those results obtained from correlations 8 and 15 with a deviation of 2.6–7.4%.

Further verification was carried out for the case of nanofluid flow in the pipe by comparing the experimental measurement Nu results with correlation 9 prediction Nu results, as shown in **Figure 16**. Very good agreement between the experimental and correlation results was demonstrated. The predicted results of Nu by the correlation are higher than the experimental results of Nu. As Re increased, a slight increase in the margin of error was observed.
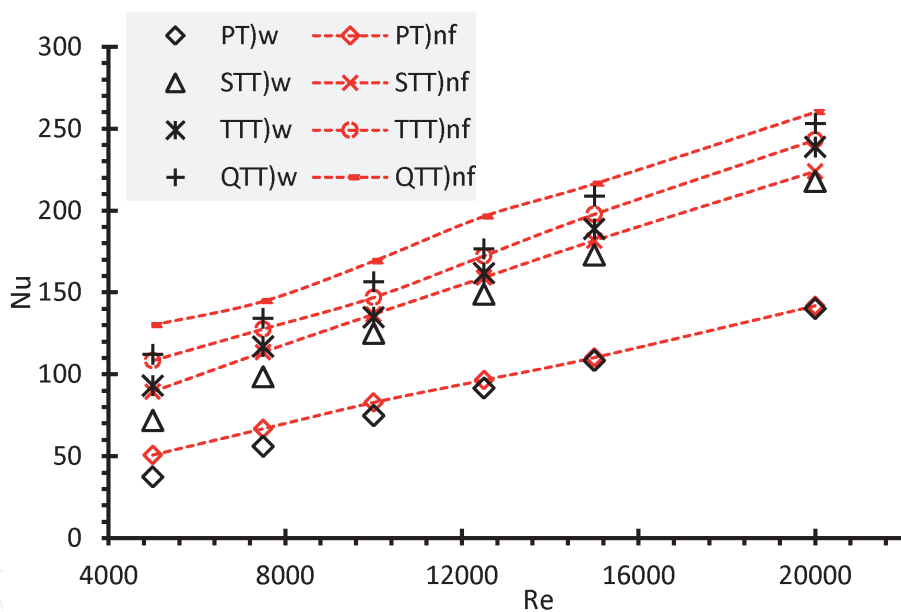
The variations of Nusselt number with Reynolds number for the tubes with different twisted tape inserts are compared in **Figure 17** for both nanofluid and base fluid. It can generally be observed that the Nusselt number increases as the Reynolds number increases. This arises as a result of the momentum that overcomes the viscous force of the fluid as the Reynolds number increases and in effect diminishes the shear between the fluid and the tube wall.

plane tube

tube with single insert

Figure 15.
Verification of experimental results for heat exchange performance by: (a) comparison with Gnielinski correlation for water flow in plain tube. (b) Comparison with Bergles correlation for water flow in tube with single TT insert.

Figure 16.
Validation of experimental results for Nusselt number to the plain tube with Duangthongsuk and Wingwiscs correlation for 0.1 vol.% TiO$_2$/water nanofluid flow.

Figure 17.
Variation of Nusselt number with Reynolds number for plain tubes and tubes with single, triple, and quintuple twisted tape inserts operating with water flow and 0.1 vol.% TiO$_2$/water nanofluid flow.

For water flow, the STT has Nusselt numbers of 43.4–63.2% higher than plain tube. This enhancement in heat transfer rate returns to the act of twisted tape that generates swirl motion, which leads to the better temperature distribution at the core region and increases turbulence intensity at near wall region that results in higher temperature gradient there and enhances heat transfer coefficient. Also, secondary flow with greater enhancement was realized at higher Reynolds numbers.

In case of water flow, Nusselt numbers of TTT and QTT are 50.12–83.74% and 57.48–100.066% higher than that in measured in PT. It is obvious that Nusselt number increases with increasing twisted tape number due to increase in secondary motion violence, which disperses the high temperature region near wall to uniformly distribute all over flow cross sectional area, which is recognized as the key factor of heat transfer enhancement.

For 0.1 vol.% TiO_2/water nanofluid flow, PT, STT, TTT, and QTT have Nusselt numbers of 1.3–30.4%, 46.1–83.2%, 53.8–97.5%, and 59.9–110.8%, respectively, higher than that in PT with water flow. This behavior is due to the fact that nanoparticles presented in the base liquid increase the thermal conductivity, which leads to an increase in heat transfer performance.

6. Conclusions

Heat transfer and fluid flow characteristics through tubes induced with multiple plain twisted tape inserts using water and 0.1 vol.% TiO_2/water nanofluid were investigated experimentally and numerically. The investigations were carried out for turbulent flow with Reynolds number ranging between 5000 and 20,000. The findings may be summarized as follows:

- It is found that tube fitted with quintuple twisted tape inserts performed highest in augmenting heat transfer. Nusselt numbers obtained by using quintuple twisted tapes inserts are up to 110.8% for nanofluid flow and 100.0% for water flow higher than in plain tube with water flow.

- As the number of twisted tapes increases, higher Nusselt number is obtained, compared to plain tube.

- The pressure drop and friction factor increase significantly by using twisted tape inserts and slightly by nanofluid.

- Using nanofluids with twisted tape inserts are resulting in more heat transfer augmentation than using each one individually.

- Using twisted tape inserts need to increase fluid pumping power due to high pressure drop produced. When using nanofluid without inserts, pumping power is not affected as the increase in the pressure drop is negligible compared to the case of pure water flow.

Accordingly, the combined technique of twisted tape inserts and nanofluid is recommended for heat exchanger application, as the heat transfer is considerably enhancing, with reasonable penalty in pumping power.

Acknowledgements

Abbreviations

D	tube diameter (mm)
f	friction factor

I	turbulence intensity
K	thermal conductivity (W/m•K)
L	tube length (mm)
Nu	Nusselt number
Δp	pressure drop (Pa)
Pr	Prandtl number
$\overset{=}{q}$	heat flux (W/m^2)
Re	Reynolds number
V	mean velocity (m/s)
w	tape width (mm)
y	tape pitch 180° (mm)
δ	tape thickness (mm)
v	kinematic viscosity (m^2/s)
φ	nanoparticles volume fraction (%)
ρ	fluid density (kg/m^3)
μ	fluid dynamic viscosity (kg/m s)
c_p	fluid-specific heat (J/kg•K)

Subscripts

b	bulk
h	hydraulic
in	inlet
nf	nanofluid
s	surface
w	water

Acronyms

PT	plain tube
STT	tube with single twisted tape
TTT	tube with triple twisted tapes
QTT	tube with quintuple twisted tapes

Author details

Hussain H. Al-Kayiem[1*], Muna S. Kassim[2] and Saud T. Taher[2]

1 Mechanical Engineering Department, Universiti Teknologi PETRONAS, Perak, Malaysia

2 Mechanical Engineering Department, Al-Mustansiriyah University, Baghdad, Iraq

*Address all correspondence to: hussain_kayiem@utp.edu.my

IntechOpen

References

[1] Kakaç S, Liu H. Heat Exchangers: Selection, Rating and Thermal Design. 2nd ed. USA, New York: CRC Press LLC, Taylor & Francis Inc.; 2002

[2] Kumar CN, Murugesan P. Review on twisted tapes heat transfer enhancement. International Journal of Science & Engineering Research. 2012;**3**(4):1-9

[3] Al-Kayiem HH, Saw CL, Afolabi L. Review on nanomaterials for thermal energy storage technologies. Journal of Nanoscience and Nanotechnology. 2013;**3**:60-71. DOI: 10.2174/2211352513119990011

[4] Dey D, Kumar P, Samantaray S. A review of nanofluid preparation, stability, and thermo-physical properties. Heat Transfer - Asian Research. 2017;**46**(8):1413-1442. DOI: 10.1002/htj.21282

[5] Ali N, Teixeira JA, Addali A. A review on nanofluids: Fabrication, stability, and thermophysical properties. Journal of Nanomaterials. 2018;**2018**: 6978130. DOI: 10.1155/2018/6978130

[6] Narayanan MV, Rakesh SG, Nanofluids SG. A review on current scenario and future prospective. IOP Conference Series: Materials Science and Engineering. 2018;**377**:012084. DOI: 10.1088/1757-899X/377/1/012084

[7] Said Z, Saidur R, Hepbasli A, Rahim NA. New thermophysical properties of water based TiO_2 nanofluid-the hysteresis phenomenon revisited. International Communications in Heat and Mass Transfer. 2014;**58**:85-95. DOI: 10.1016/j.icheatmasstransfer.2014.08.034

[8] He Y, Men Y, Zhao Y, Lu H, Ding Y. Numerical investigation into the convective heat transfer of TiO_2 nanofluids flowing through a straight tube under the laminar flow conditions. Applied Thermal Engineering. 2009;**29**: 1965-1972. DOI: 10.1016/j.applthermaleng.2008.09.020

[9] Bergles AE, Manglik RM. Heat transfer and pressure drop correlations for twisted tape inserts in isothermal tube: Part II-transition and turbulent flows. Transaction of ASME Journal of Heat Transfer. 1993;**115**:890-896. DOI: 10.1115/1.2911384

[10] Bhattacharyya S, Saha S, Saha SK. Laminar flow heat transfer enhancement in a circular tube having integral transverse rib roughness and fitted with centre-cleared twisted-tape. Experimental Thermal and Fluid Science. 2013;**44**:727-735. DOI: 10.1016/j.expthermflusci.2012.09.016

[11] Bhattacharyya S, Chattopadhyay H, Benim AC. Simulation of heat transfer enhancement in tube flow with twisted tape insert. Progress in Computational Fluid Dynamics An International Journal. 2017;**17**(3):193-197. DOI: 10.1504/PCFD.2017.084356

[12] Bhattacharyya S, Chattopadhyay H, Benim AC. Computational investigation of heat transfer enhancement by alternating inclined ribs in tubular heat exchanger. Progress in Computational Fluid Dynamics, An International Journal. 2017;**17**(6):390-396. DOI: 10.1504/PCFD.2017.088818

[13] Bhattacharyya S, Benim AC, Chattopadhyay H, Banerjee A. Experimental investigation of heat transfer performance of corrugated tube with spring tape inserts. Experimental Heat Transfer. 2018;**32**(5):411-425. DOI: 10.1080/08916152.2018.1531955

[14] Pourrajabi M, Nezhad AR, Pourrajabi MR. Numerical study of turbulent flow and heat transfer of a nanofluid in a circular tube with twisted

tape insert. In: International Symposium on Advances in Science and Technology. Iran: 7th SASTech; 2013. DOI: 10.1007/s10973-017-6900-5

[15] Maddah H, Farokhi M, Aghayari R, Jahanizadeh S, Ashtary K. Effect of twisted-tape turbulator and nanofluid on heat transfer in a double pipe heat exchanger. Journal of Engineering. 2014;**2014**:920970. DOI: 10.1155/2014/920970

[16] Safikhani H, Eiamsa-ard S. Multi-objective optimization of TiO_2-water nanofluid flow in tubes fitted with multiple twisted tape inserts in different arrangement. Journal of Transport Phenomena in Nano-Micro Scale. 2015; **3**(2):89-99. DOI: 10.7508/tpnms.2015.02.003

[17] Saleh FA. Computational and experimental investigations on thermal and fluid flow characteristics for different models of tapes inserts with TiO_2/water nanofluid under turbulent conditions. International Journal of Mechanical & Mechatronics Engineering. 2018;**19**(2):1-14

[18] Eiamsa-ard S, Wongcharee K. Convective heat transfer enhancement using Ag-water nanofluid in a micro-fin tube combined with non-uniform twisted tape. International Journal of Mechanical Sciences. 2018;**146–147**: 337-335. DOI: 10.1016/j.ijmecsci.2018.07.040

[19] Xu C, Xu S, Wei S, Chen P. Experimental investigation of heat transfer for pulsating flow of GOPs-water nanofluid in a microchannel. International Communications in Heat and Mass Transfer. 2020;**110**:104403. DOI: 10.1016/j.icheatmasstransfer.2019.104403

[20] Chun BH, Kang HU, Kim SH. Effect of alumina nanoparticles in the fluid on heat transfer in double-pipe heat exchanger system. Korean Journal of Chemical Engineering. 2008;**25**(5): 966-971. DOI: 10.1007/s11814-008-0156-5

[21] Duangthongsuk W, Wongwises S. Effect of thermophysical properties models on the predicting of the convective heat transfer coefficient for low concentration nanofluid. International Communications in Heat and Mass Transfer. 2008;**35**(10): 1320-1326. DOI: 10.1016/j.icheatmasstransfer.2008.07.015

[22] Santra AK, Sen S, Chakraborty N. Study of heat transfer due to laminar flow of copper-water nanofluid through two isothermally heated parallel plates. International Journal of Thermal Sciences. 2009;**48**(2): 391-400. DOI: 10.1016/j.ijthermalsci.2008.10.004

[23] Namburu PK, Das DK, Tanguturi KM, Vajjha RS. Numerical study of turbulent flow and heat transfer characteristics of nanofluids considering variable properties. International Journal of Thermal Sciences. 2009;**48**(2):290-302. DOI: 10.1016/j.ijthermalsci.2008.01.001

[24] Available from: https://www.visualcapitalist.com/ [Retrieved on: 26 May 2020]

[25] Pak BC, Cho YI. Hydrodynamic and heat transfer study of dispersed fluids with submicron metallic oxide particles. Experimental Heat Transfer 1998; **11**(2):151-170. DOI:10.1080/08916159808946559

[26] Batchelor GK. The effect of Brownian motion on the bulk stress in the suspension of spherical particles. Journal of Fluid Mechanics. 1977;**83**(1):97-117. DOI: 10.1017/S0022112077001062

[27] Incropera FP, DeWitt PD, Bergman TL, Lavine AS. Fundamentals of Heat and Mass Transfer. USA, New York: John-Wiley & Sons Inc.; 2006

[28] Russo F, Basse NT. Scaling of turbulence intensity for low-speed flow in smooth pipes. Flow Measurement and Instrumentation. 2016;**52**:101-114. DOI: 10.1016/j.flowmeasinst.2016.09.012